Observations and Modeling of Chromospheric Evaporation during Solar Micro-flare

Girjesh R. Gupta

Udaipur Solar Observatory
Physical Research Laboratory

Aveek Sarkar, PRL
Durgesh Tripathi, IUCAA

7 Nov, 2019

IRIS-10, Bangalore

Outline of presentation

- Introduction: Microflare and chromospheric evaporation
- Observations: IRIS, Hinode, and SDO
- Results: Intensity, velocity, density, temperature, energetics
- Comparison: 1-D hydrodynamic loop simulations
- Summary

Solar Microflares: Active-Region Transient Brightenings (ARTB)

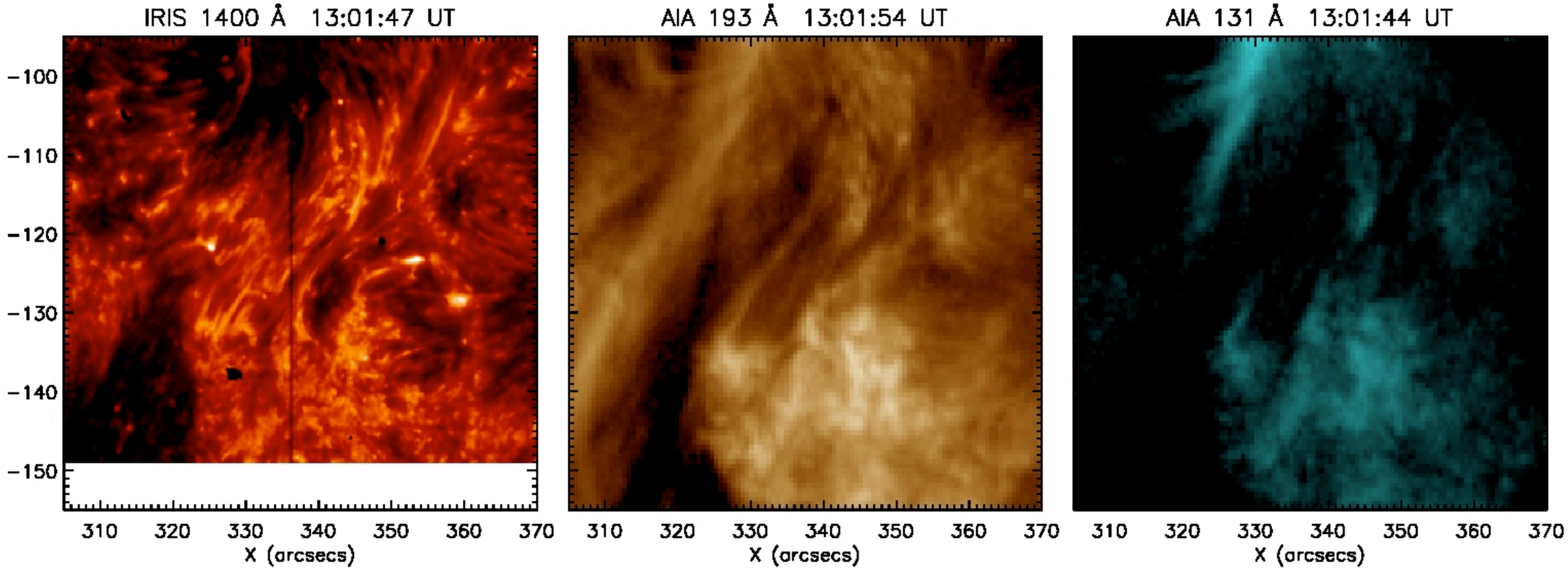

SXT/Yohkoh

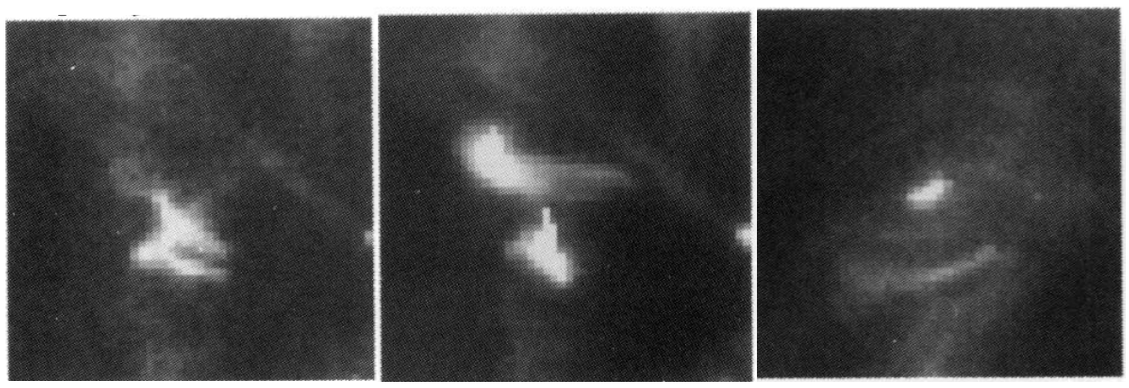

— Shimizu et al. (1994)

MORPHOLOGICAL CLASSIFICATION OF TRANSIENT BRIGHTENING

Classification	Number	%
Total analyzed event	142	
Point-like event	26	18.3
Single loop event	59	41.5
Multiple loop event	57	40.2
2 loops		
balanced intensity	30	52.6
unbalanced intensity	19	33.3
>2 loops (complicated)	8	14.1

Microflare energy: 10^{25}-10^{28} erg (Shimizu 1995) cf. solar flares: 10^{29}-10^{33} erg

Solar Microflares: Active-Region Transient Brightenings (ARTB)

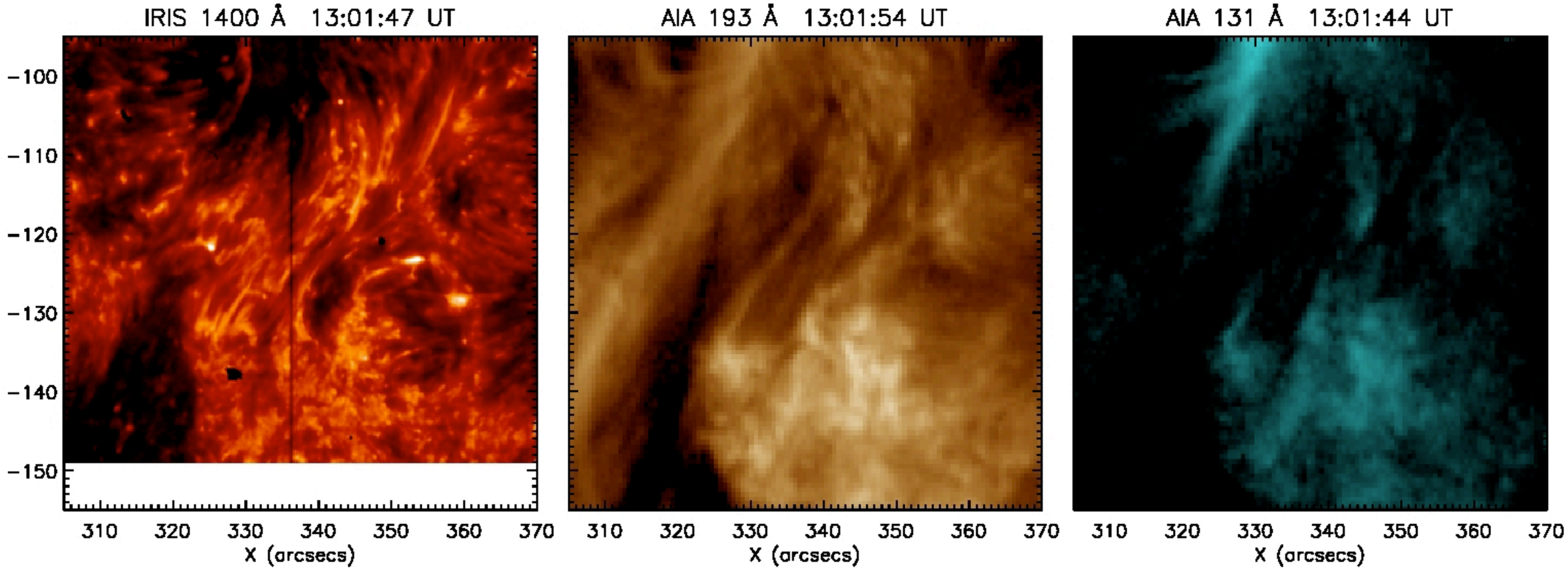

SXT/Yohkoh

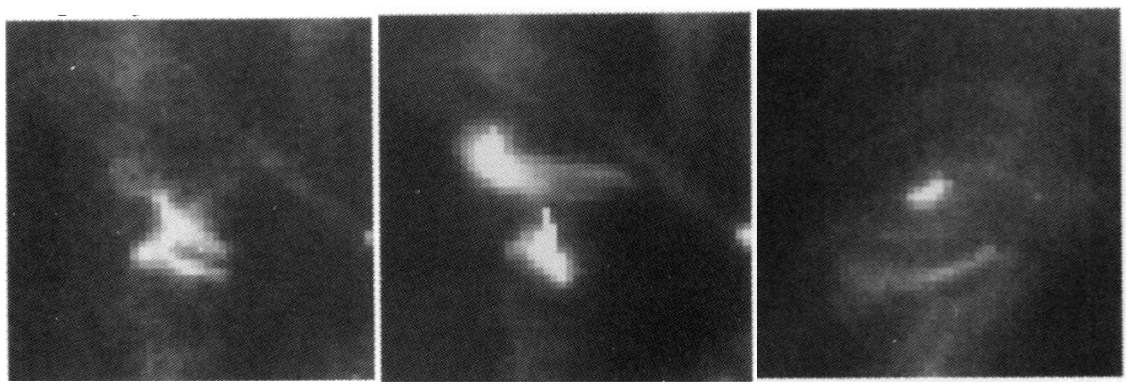

— Shimizu et al. (1994)

MORPHOLOGICAL CLASSIFICATION OF TRANSIENT BRIGHTENING

Classification	Number	%
Total analyzed event	142	
Point-like event	26	18.3
Single loop event	59	41.5
Multiple loop event	57	40.2
2 loops		
balanced intensity	30	52.6
unbalanced intensity	19	33.3
>2 loops (complicated)	8	14.1

Microflare energy: 10^{25}-10^{28} erg (Shimizu 1995) cf. solar flares: 10^{29}-10^{33} erg

Chromospheric Evaporation

- Impulsive energy released in (micro-)flares leads to heating of local chromospheric material up to very high temperatures of ≈10 MK.
- Increase in local pressure leads to chromospheric material moving upward into the corona along the (micro-)flare loops.
- This process of filling of the loop with hot plasma is called ‘chromospheric evaporation’.
- High pressure also pushes denser plasma downward into the lower chromosphere.
- Emissions from hot materials from the corona show high blueshift (upflow), and those from cool material from the upper chromosphere and transition region show small redshift (downflow) as the underlying chromosphere is denser than the overlying corona.

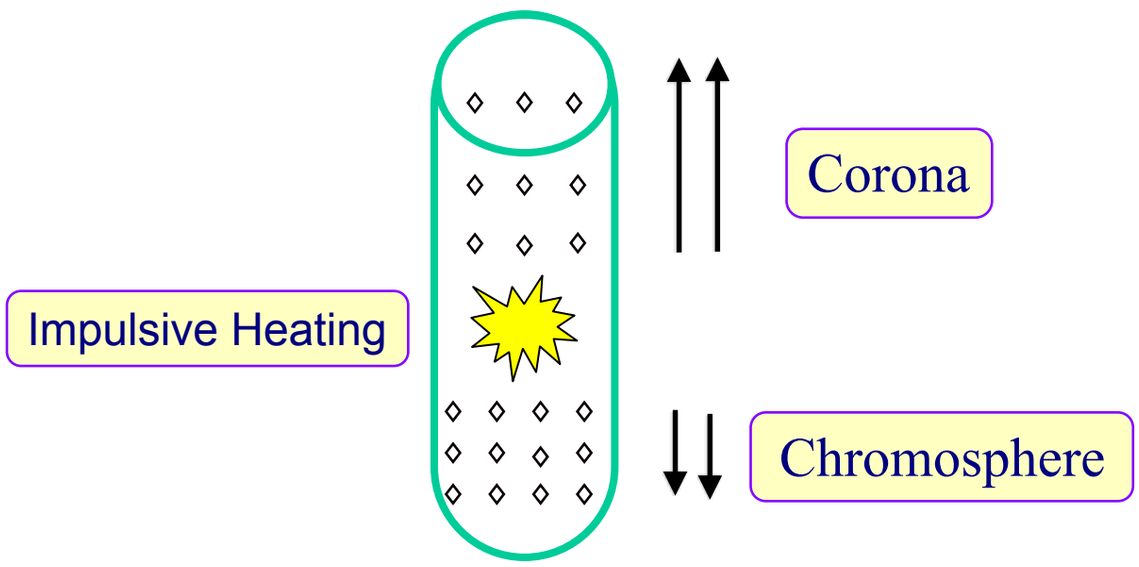

Observations

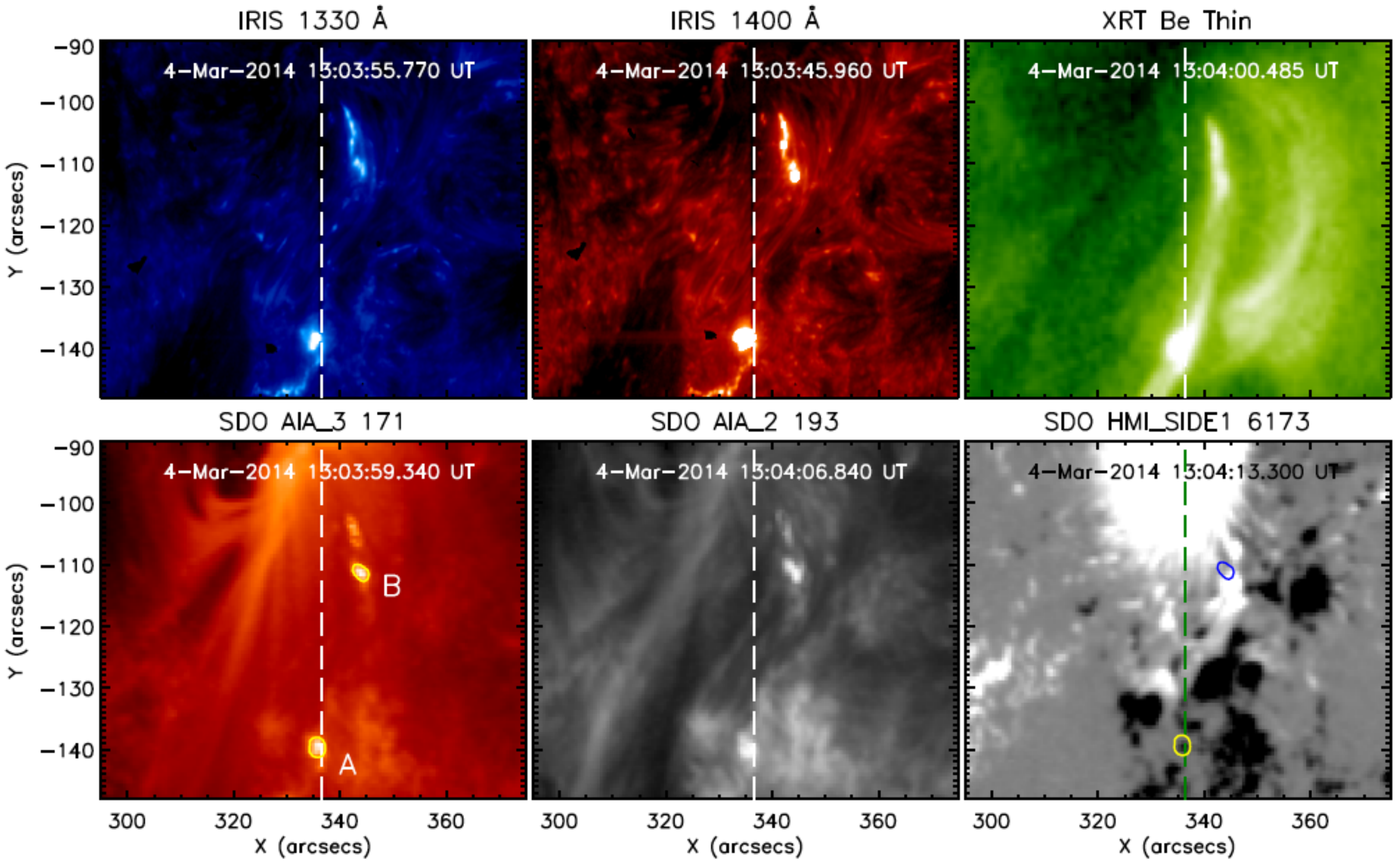

At point A, the average strength of the LOS magnetic field is about –400 G, which is surrounded by field strength of –50 G. Point B shows a strong gradient in the field strength, one-half shows a field strength of 650 G and the other half 120 G.

Line profiles: UV burst and micro-flare

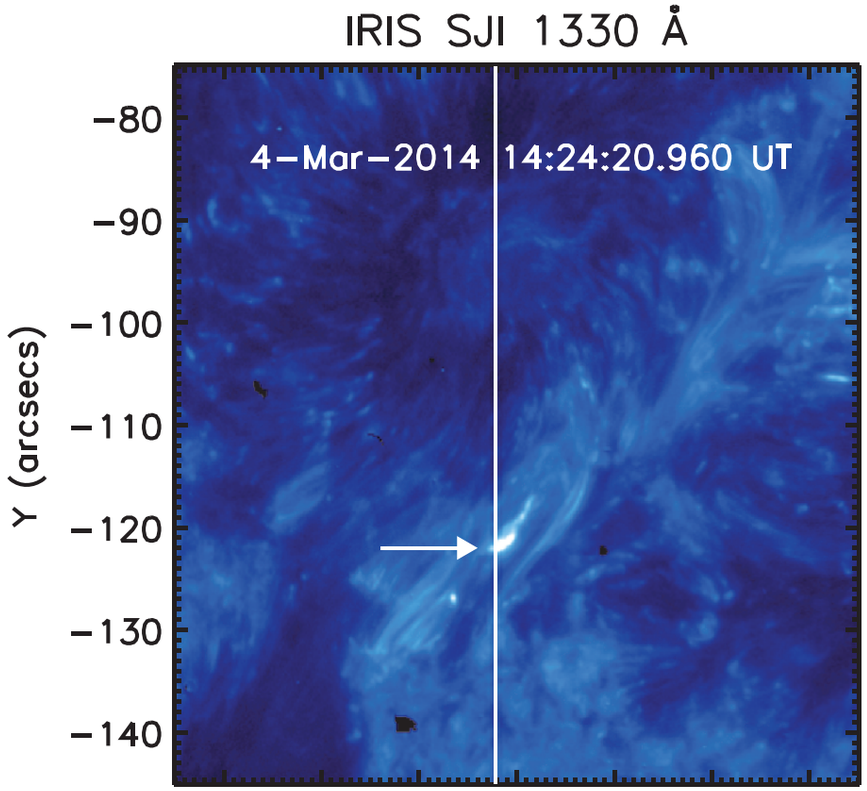

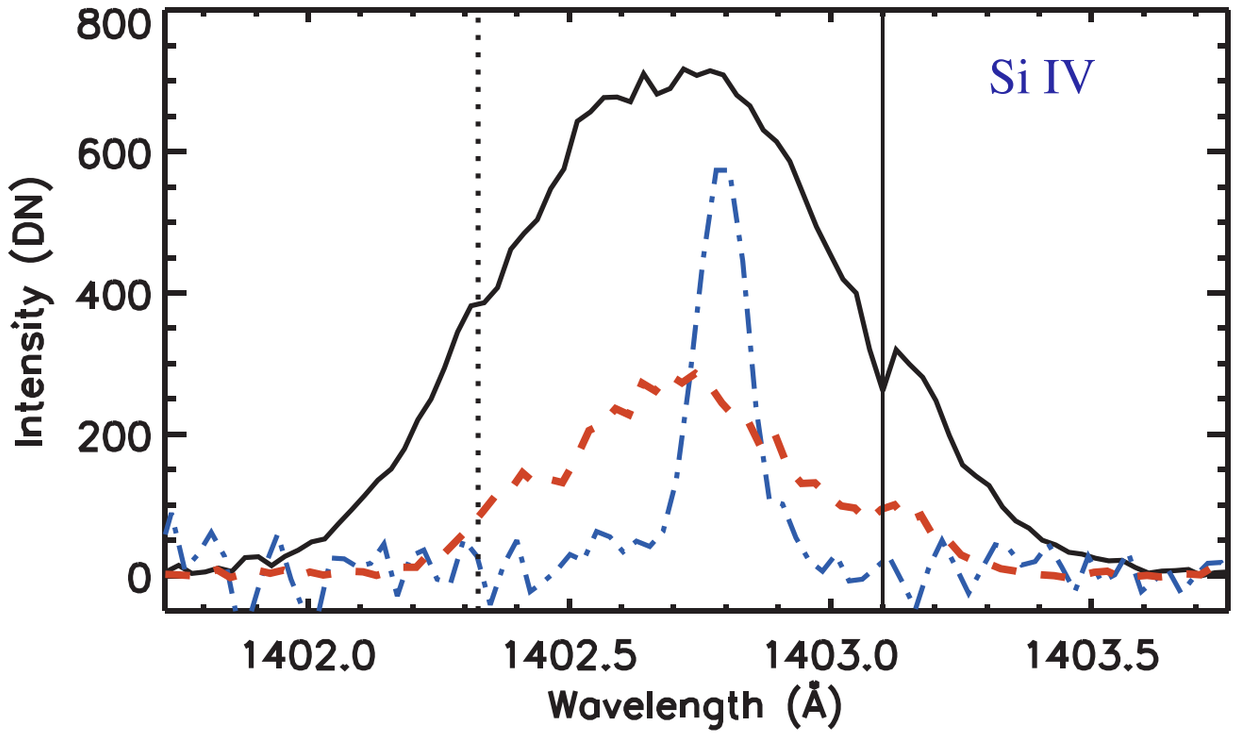

UV Burst: Broad and non-Gaussian profile

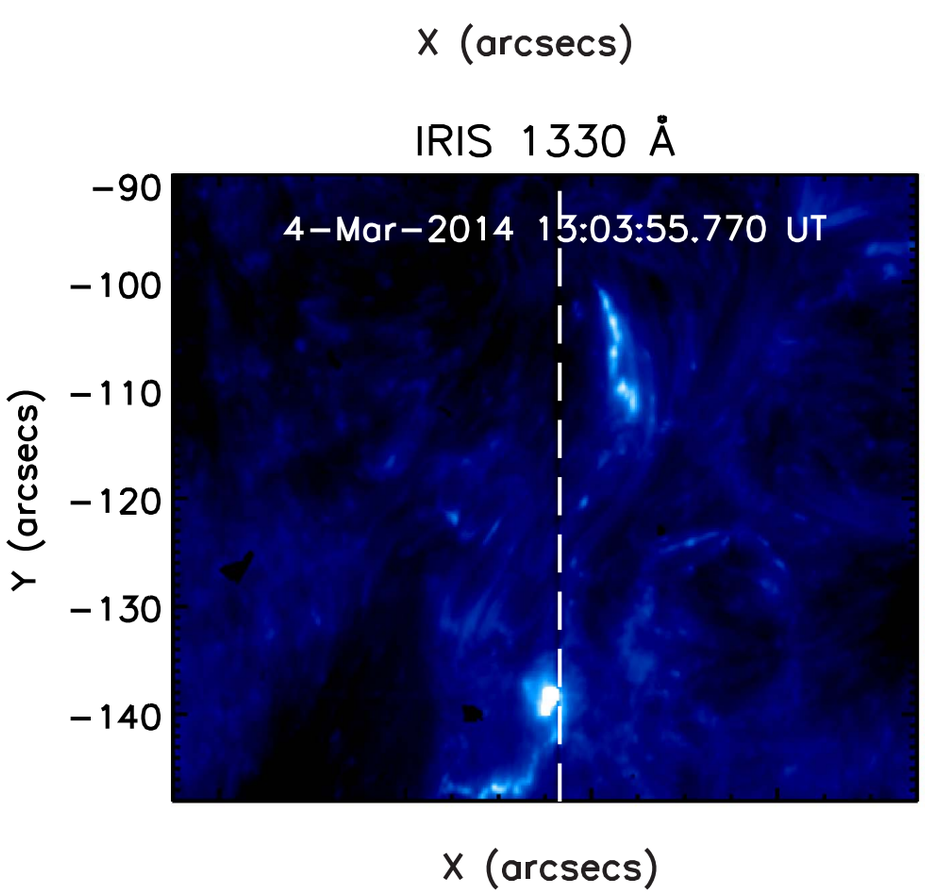

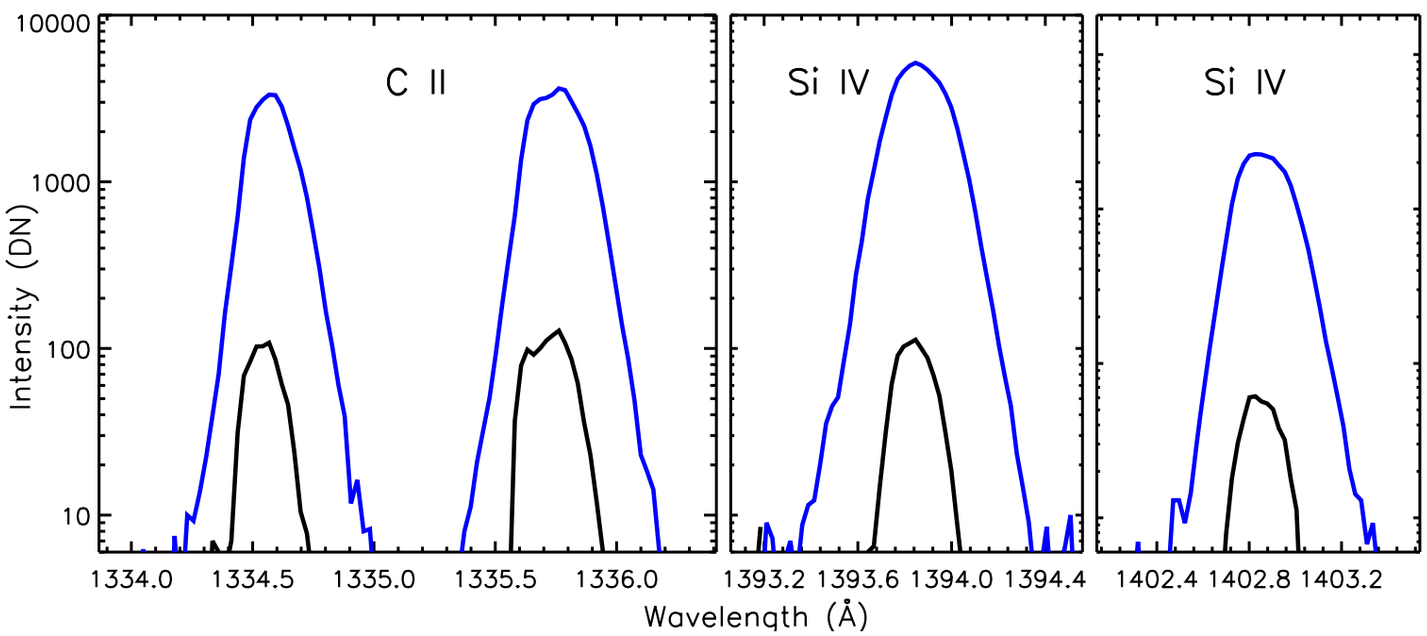

Microflare: Narrow and simple Gaussian profile

All AIA filters show micro-flare

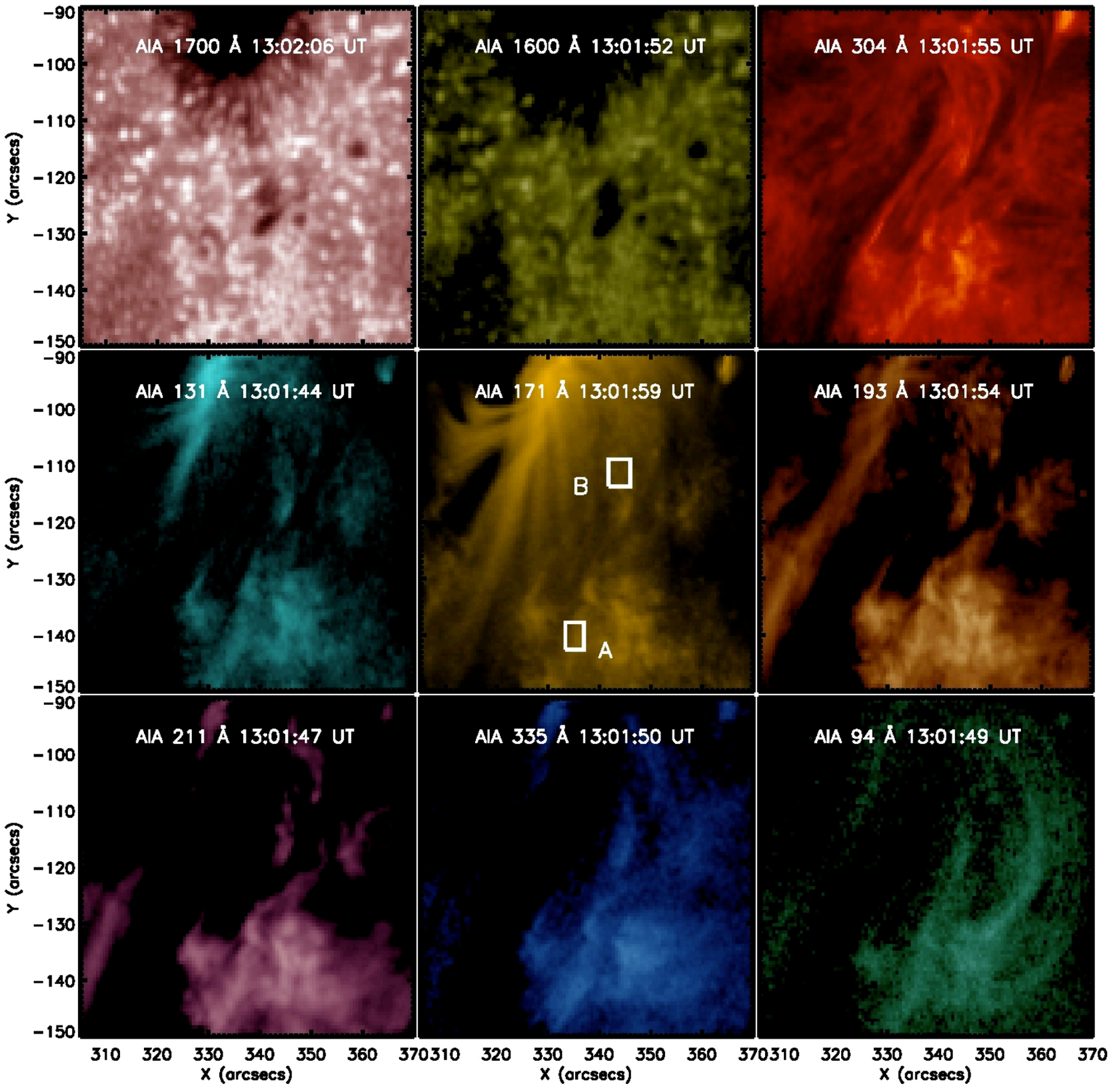

All AIA filters show micro-flare

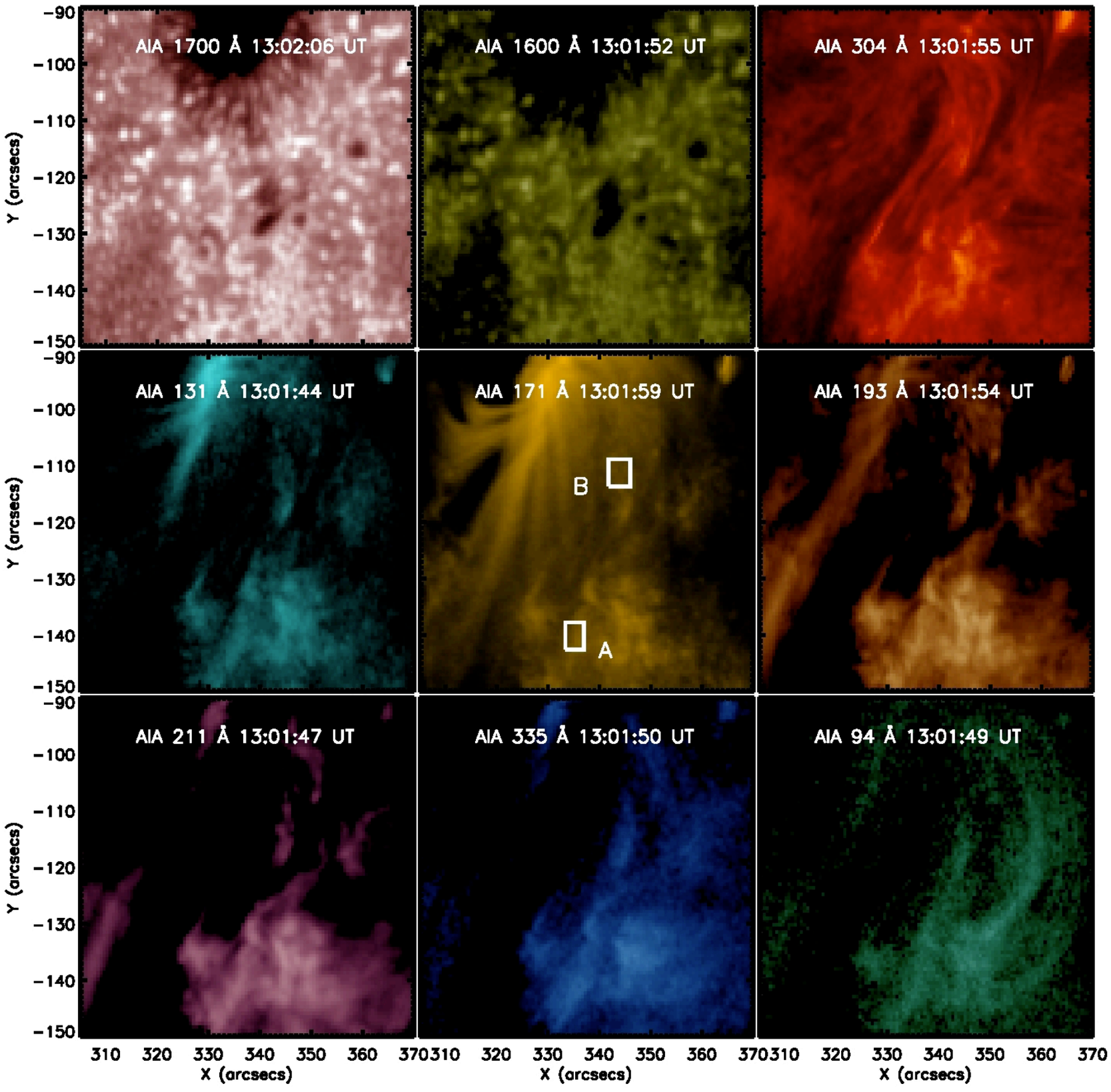

Loop brightening after micro-flare

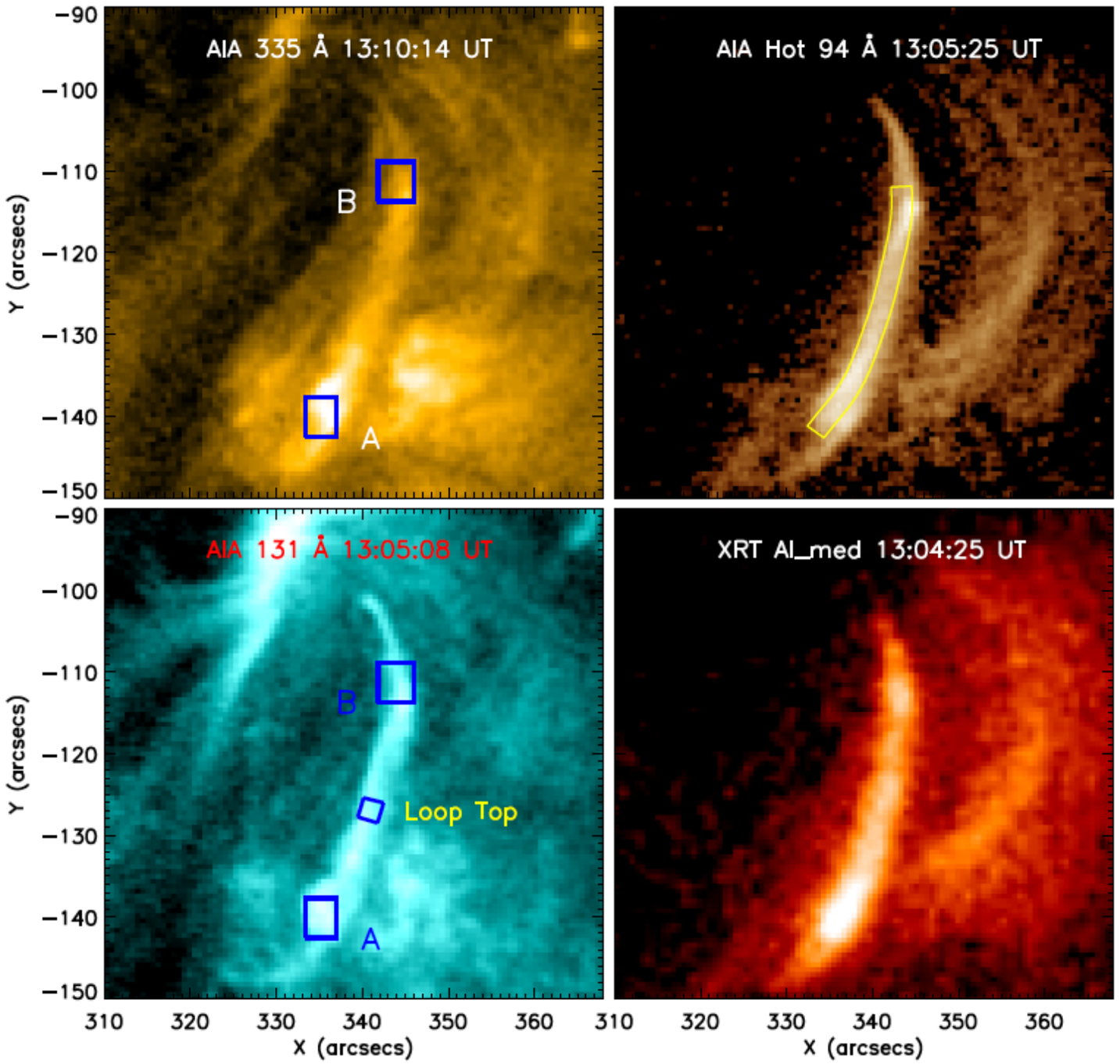

The hot plasma component from Fe XVIII 93.93 Å line from AIA 94 Å images were separated out from cool emission (Fe X and XIV) using the approach of Del Zanna (2013).

$$I(Fe\ XVIII) \approx I(94\ \text{Å}) - I(211\ \text{Å})/120 - I(171\ \text{Å})/450$$

Light curves at foot-points A & B, and loop top

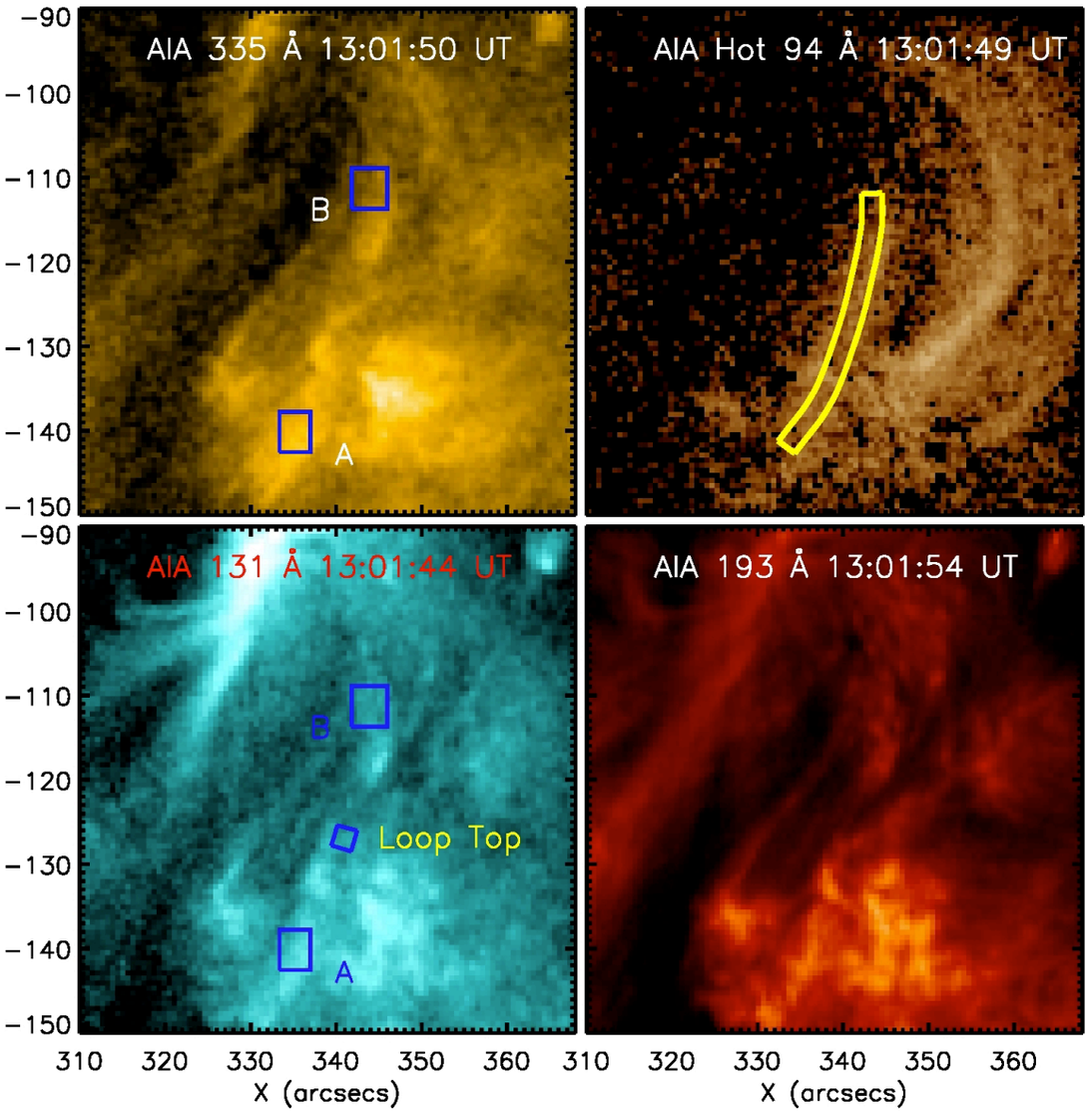

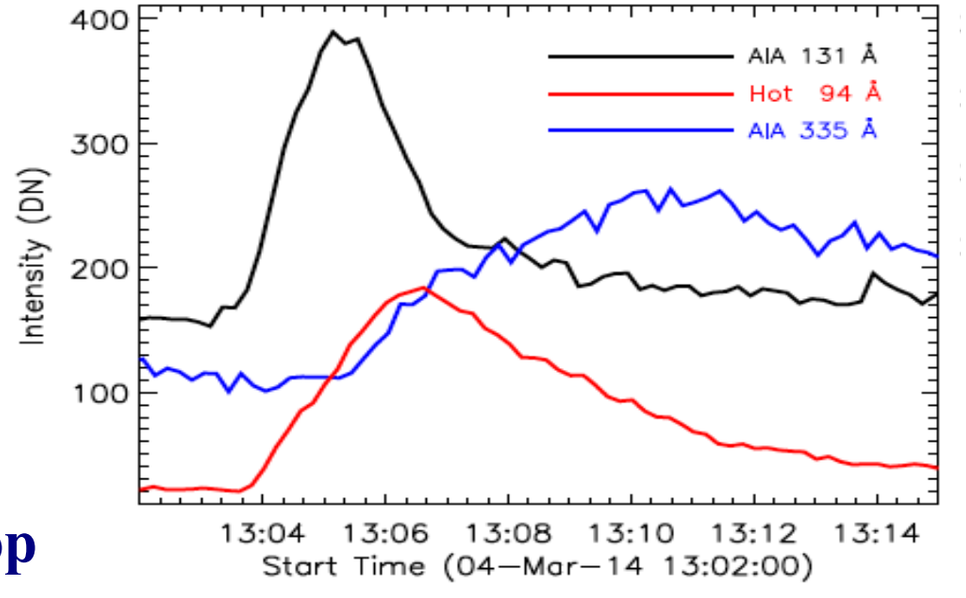

loop top

A

B

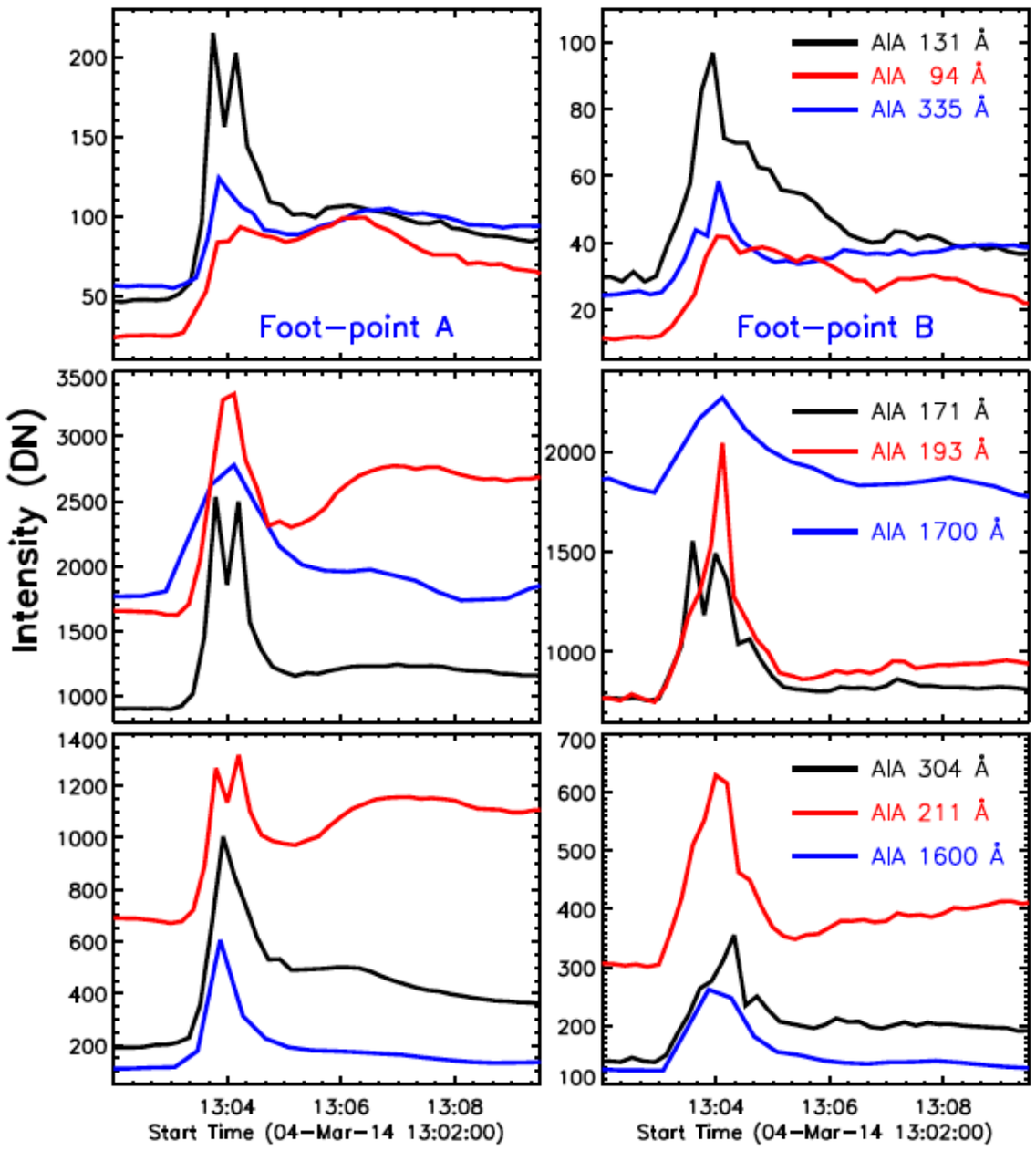

Light curves at foot-points A & B, and loop top

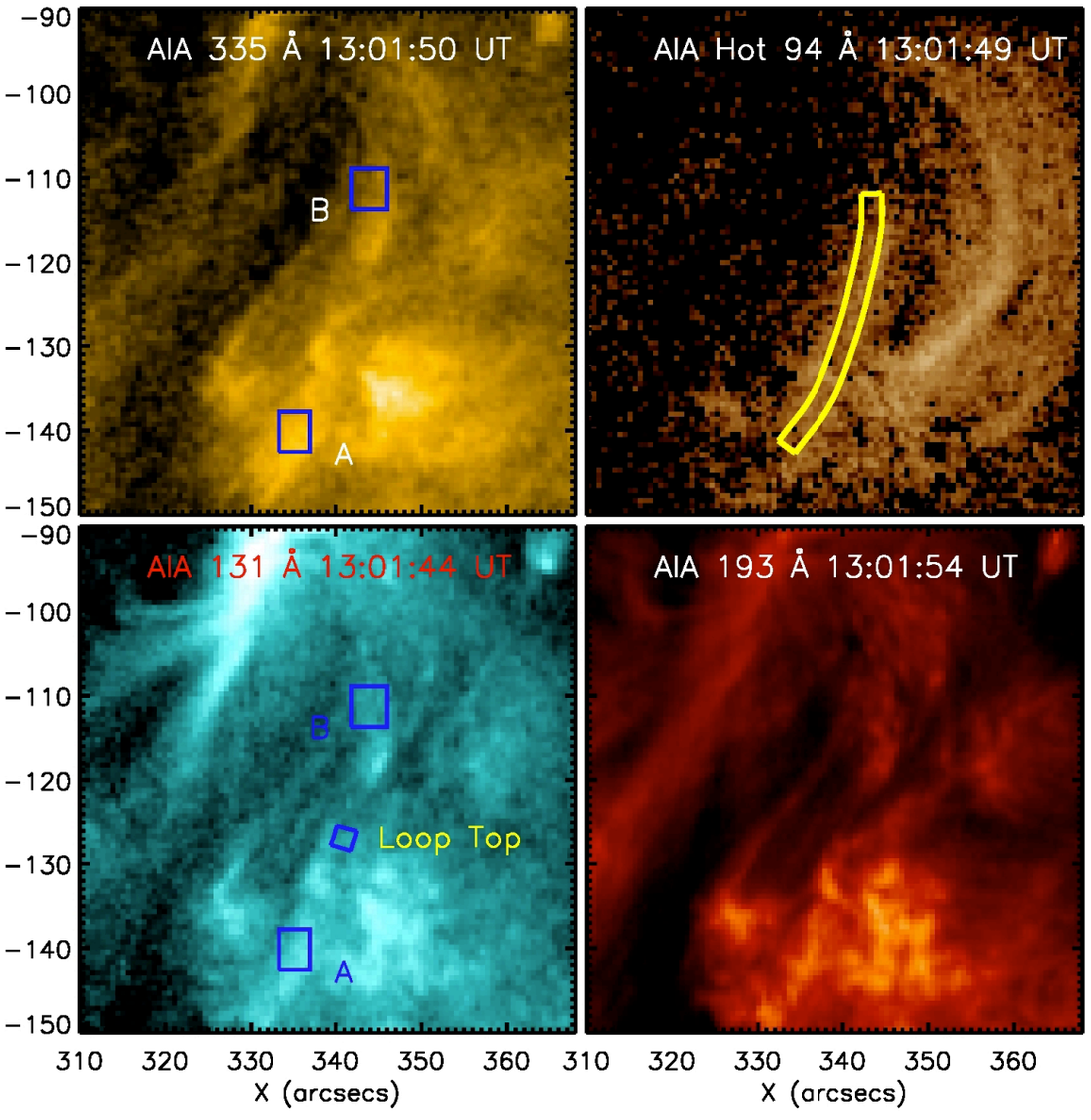

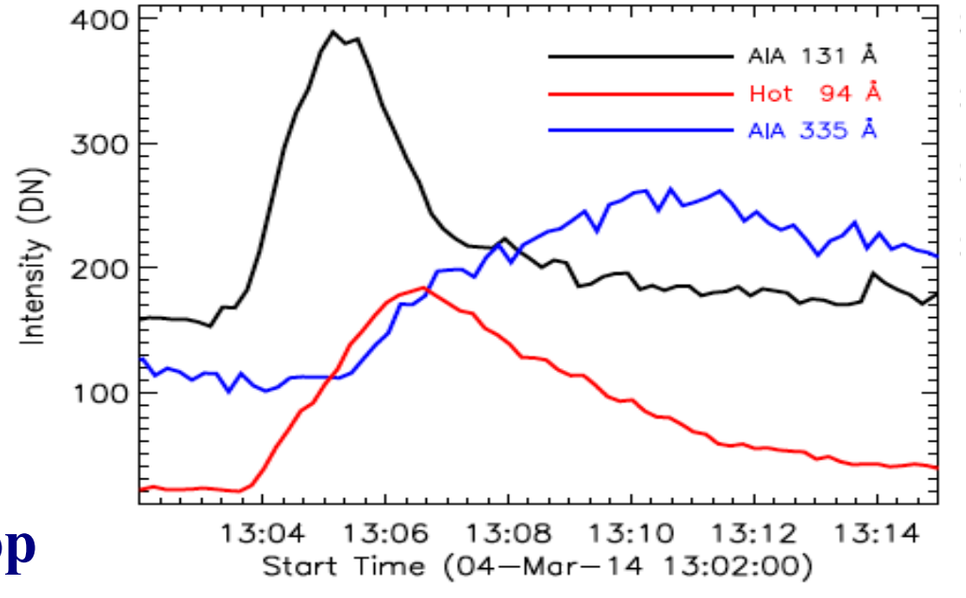

loop top

A

B

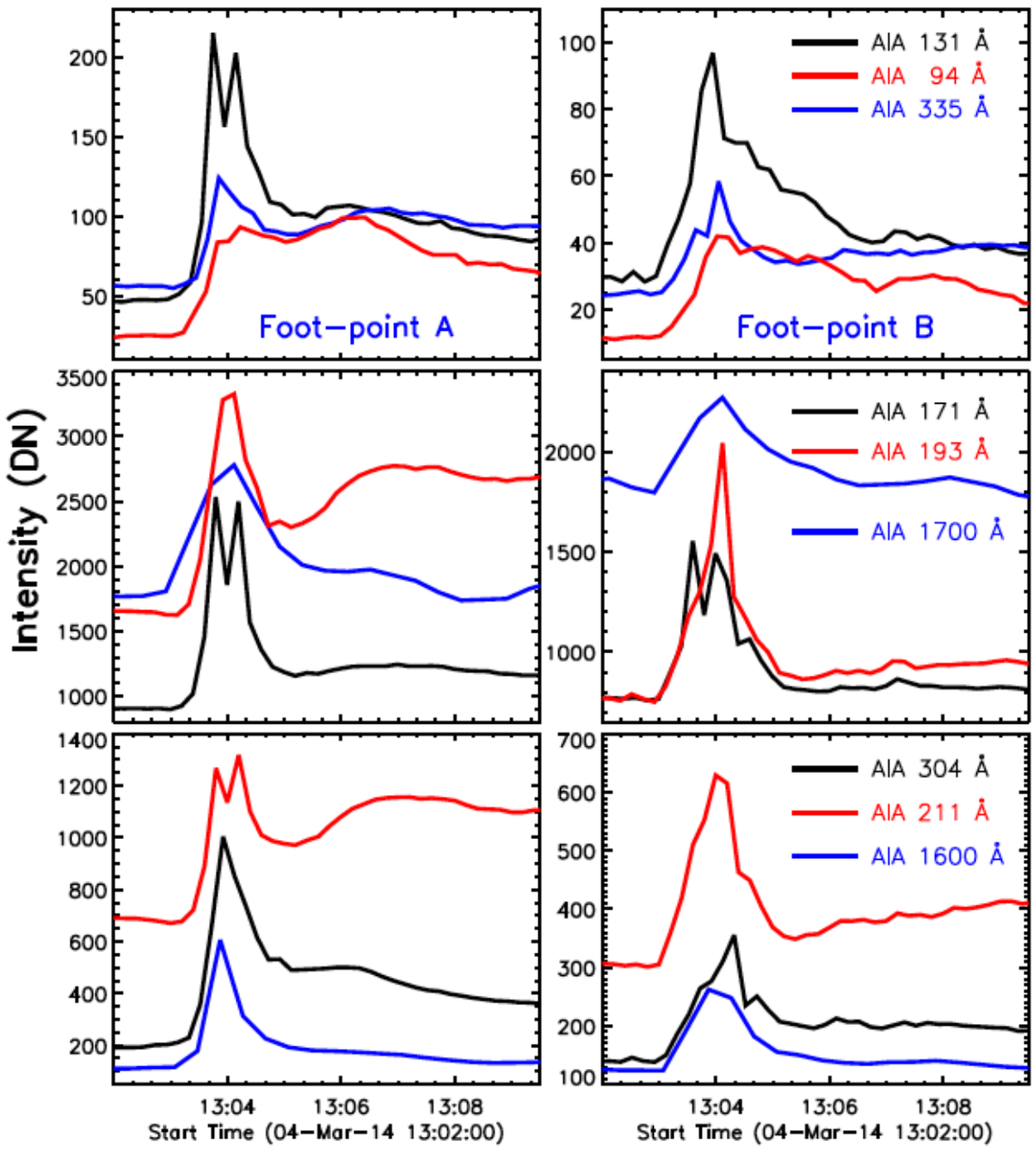

Time-distance analysis: up-flow velocity

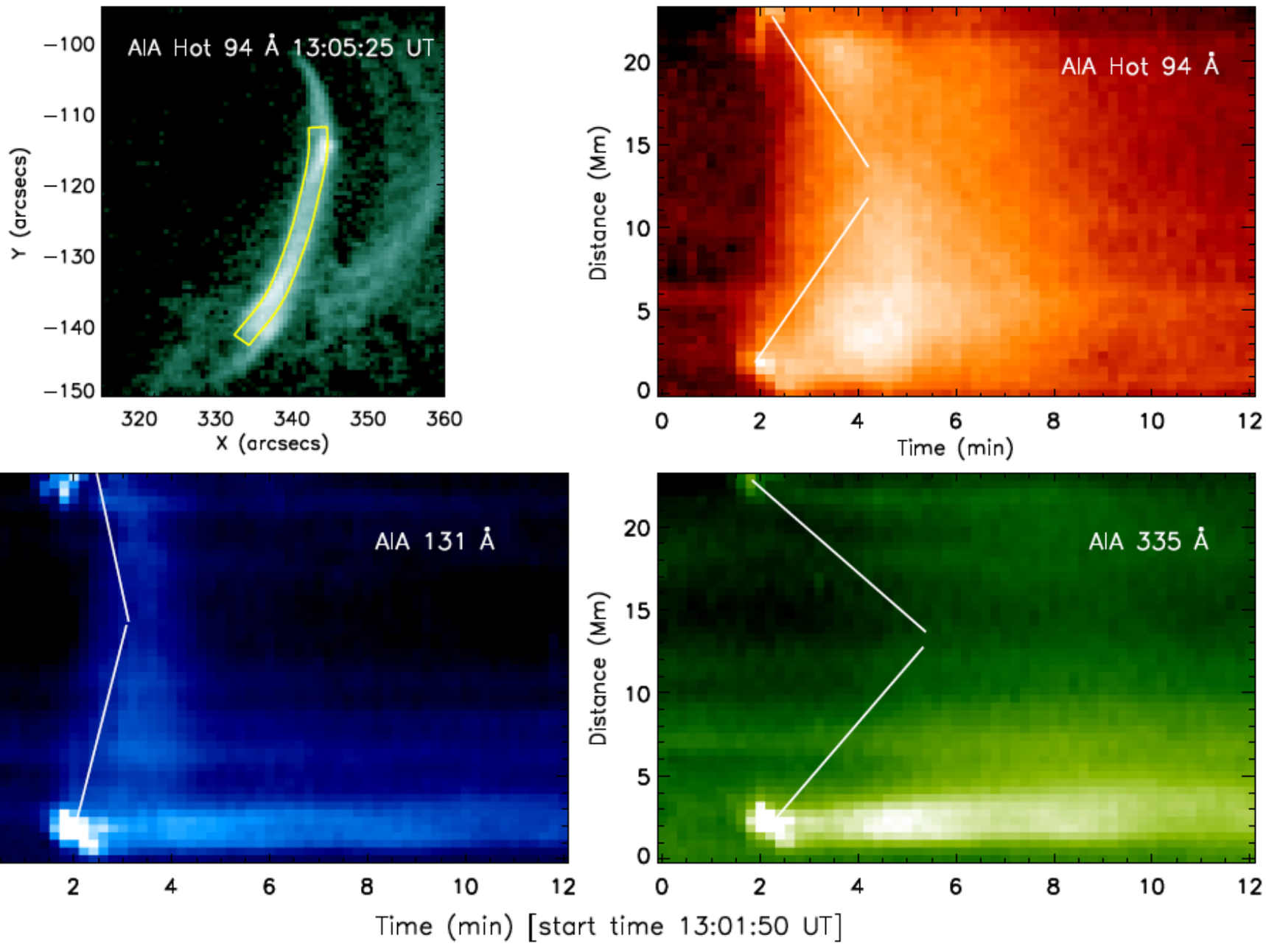

- Hot plasma moves towards the loop-top with speed 211 km/s, 74 km/s, and 50 km/s as found from AIA 131 Å, hot 94 Å, and 335 Å passbands.
- The full loop became visible after ≈ 25 s in 131 Å, ≈ 40 s in 94 Å, and ≈ 6.5 minutes in 335 Å of ARTB.

DEM Analysis: Foot-points A & B, loop top

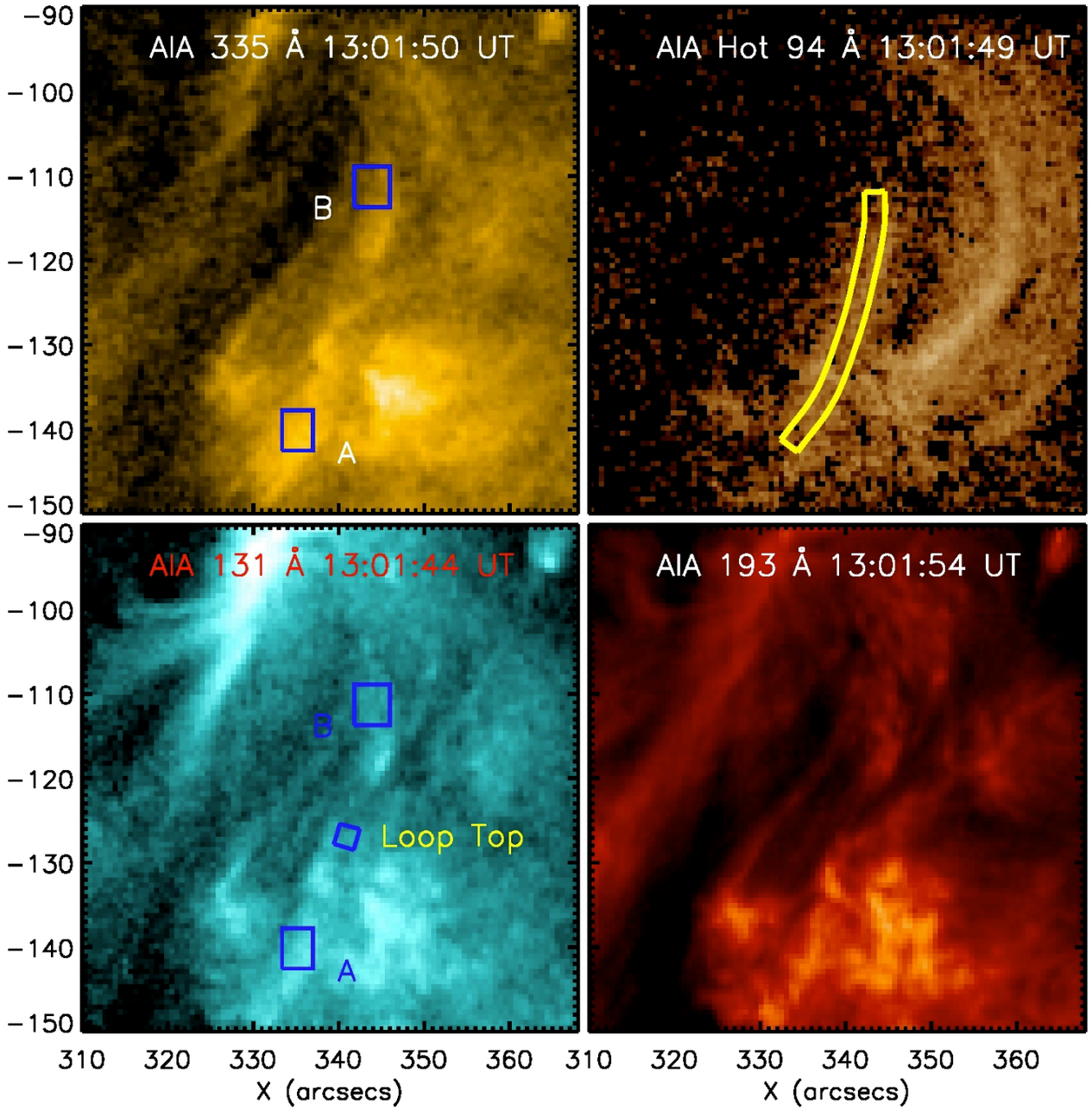

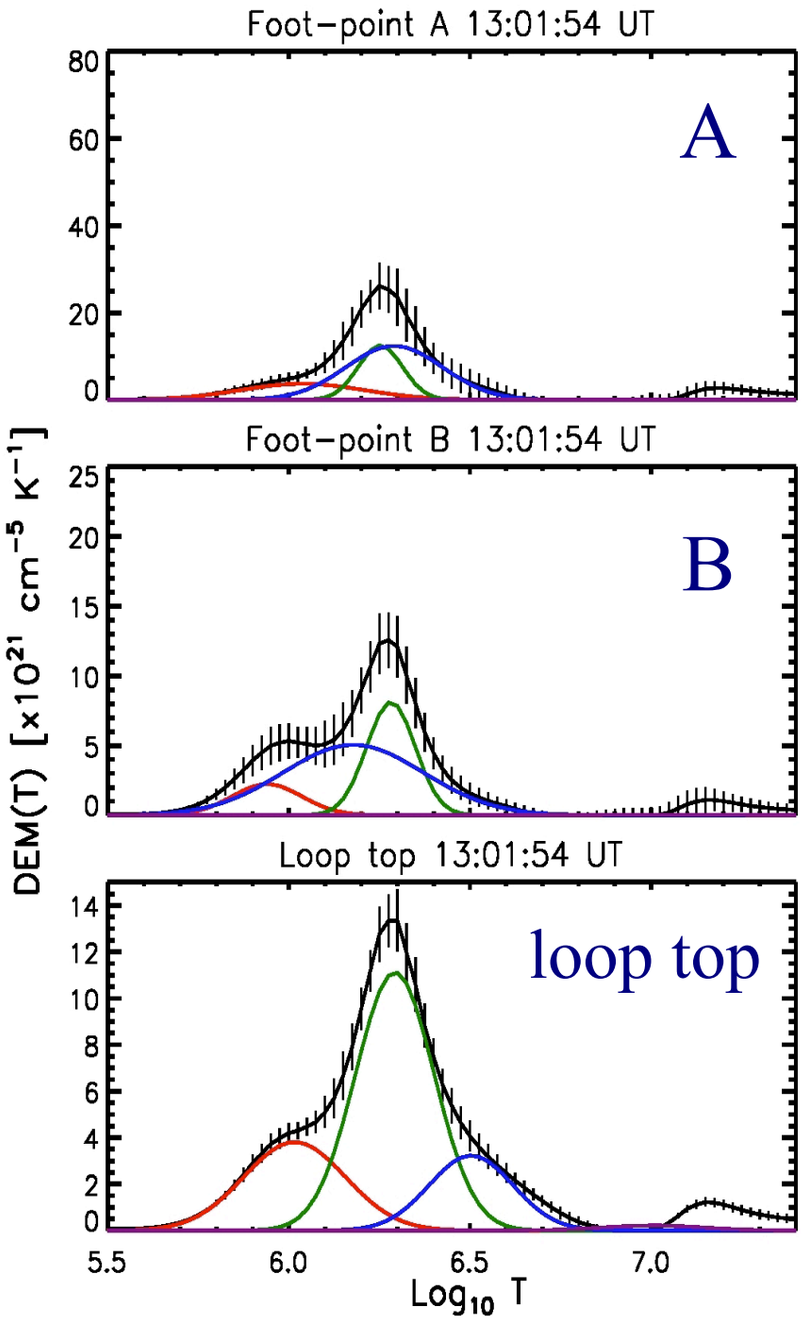

DEM profiles (from Hannah and Kontar 2012) are fitted with 4 Gaussian function. Fitted components represent cool ($10^{5.8}$–10^{6} K), warm ($10^{6.2}$–$10^{6.3}$ K), intermediate ($10^{6.2}$–$10^{6.7}$ K), and hot ($10^{6.7}$–$10^{7.2}$ K) temperature plasma components.

DEM Analysis: Foot-points A & B, loop top

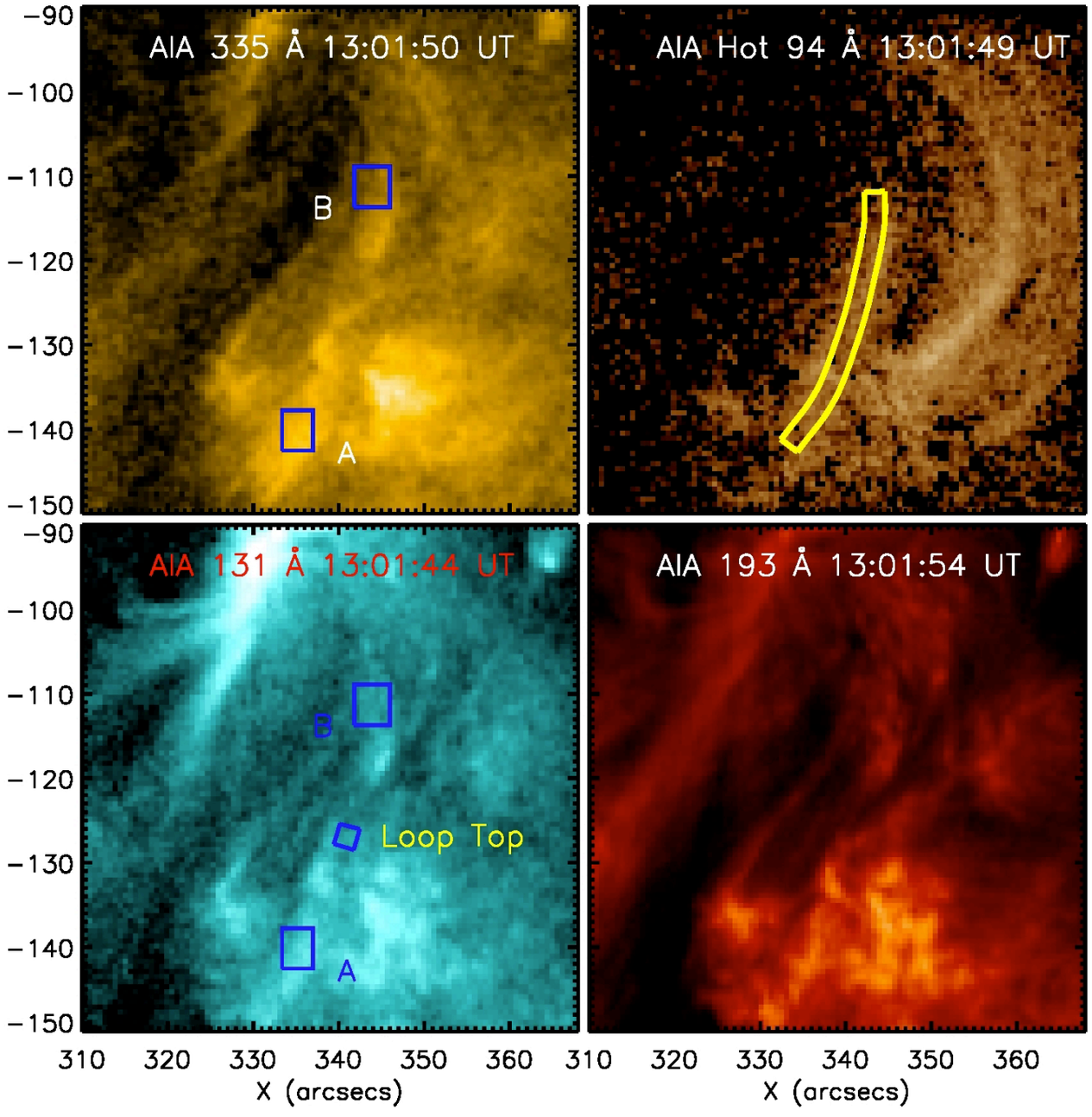

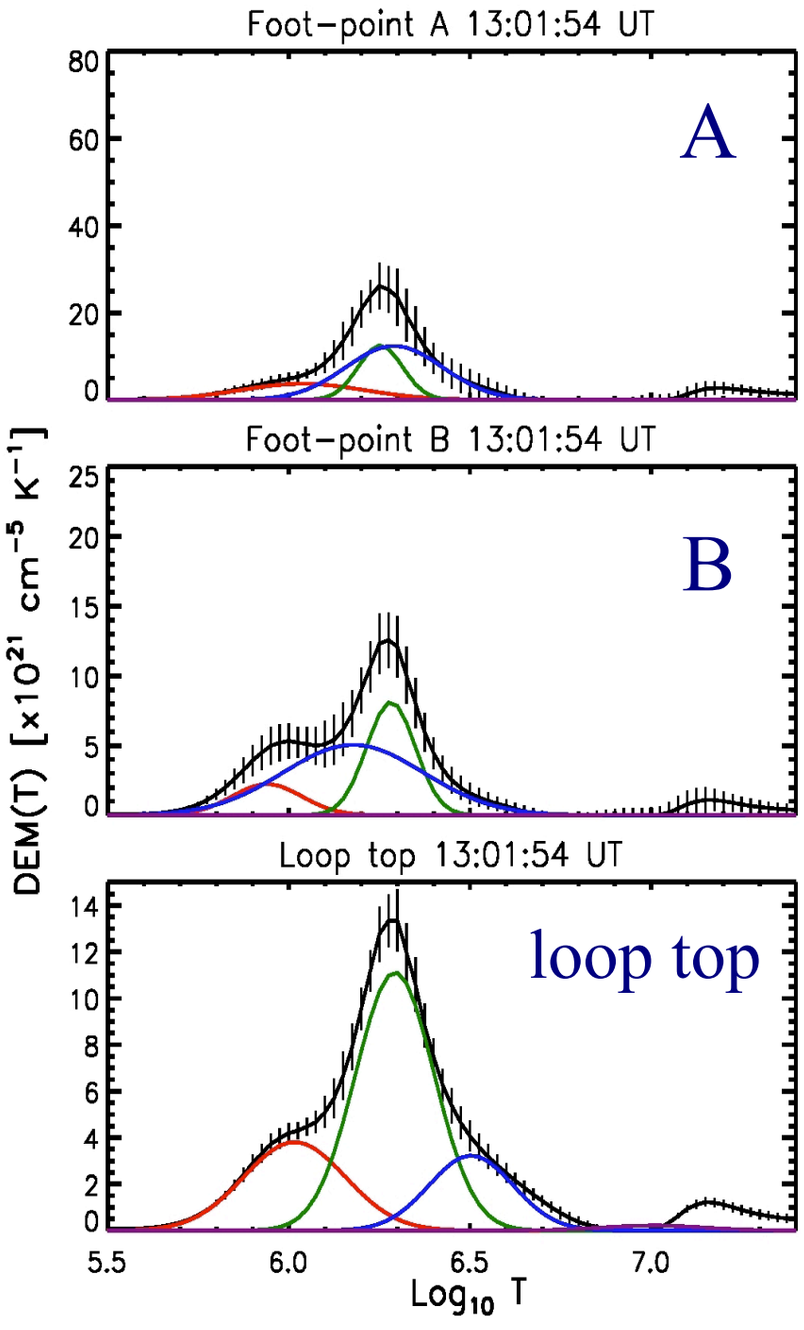

DEM profiles (from Hannah and Kontar 2012) are fitted with 4 Gaussian function. Fitted components represent cool ($10^{5.8}$–10^{6} K), warm ($10^{6.2}$–$10^{6.3}$ K), intermediate ($10^{6.2}$–$10^{6.7}$ K), and hot ($10^{6.7}$–$10^{7.2}$ K) temperature plasma components.

IRIS Spectroscopic Analysis: Density and down-flow velocity

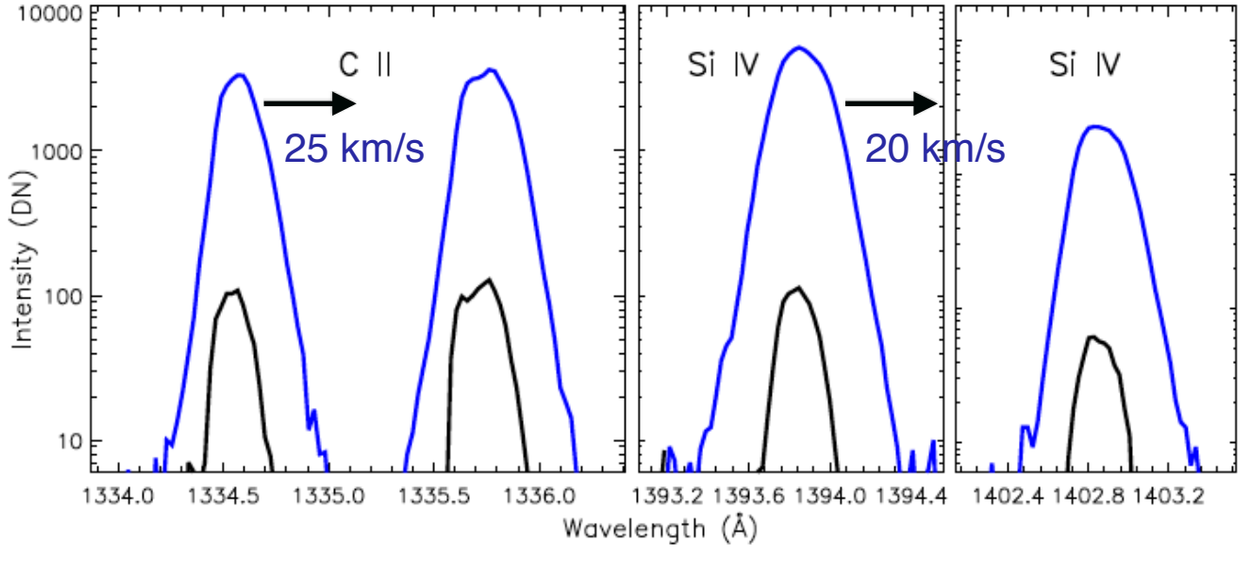

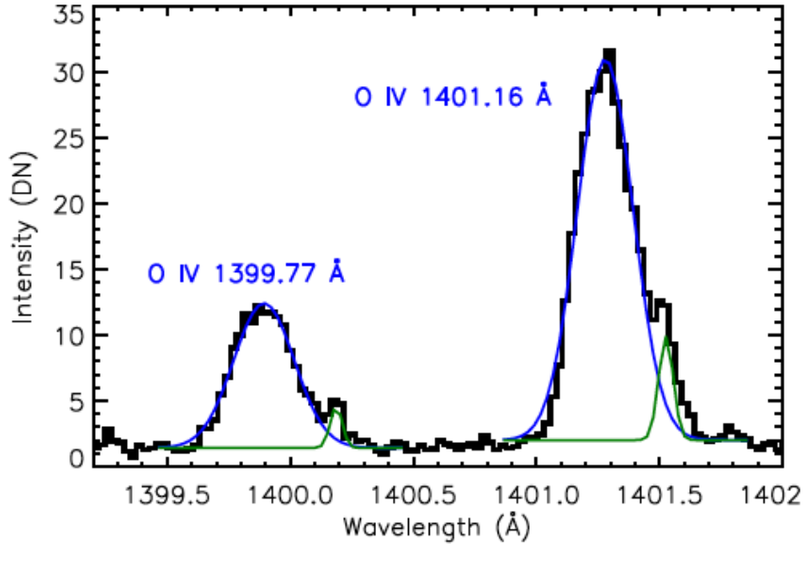

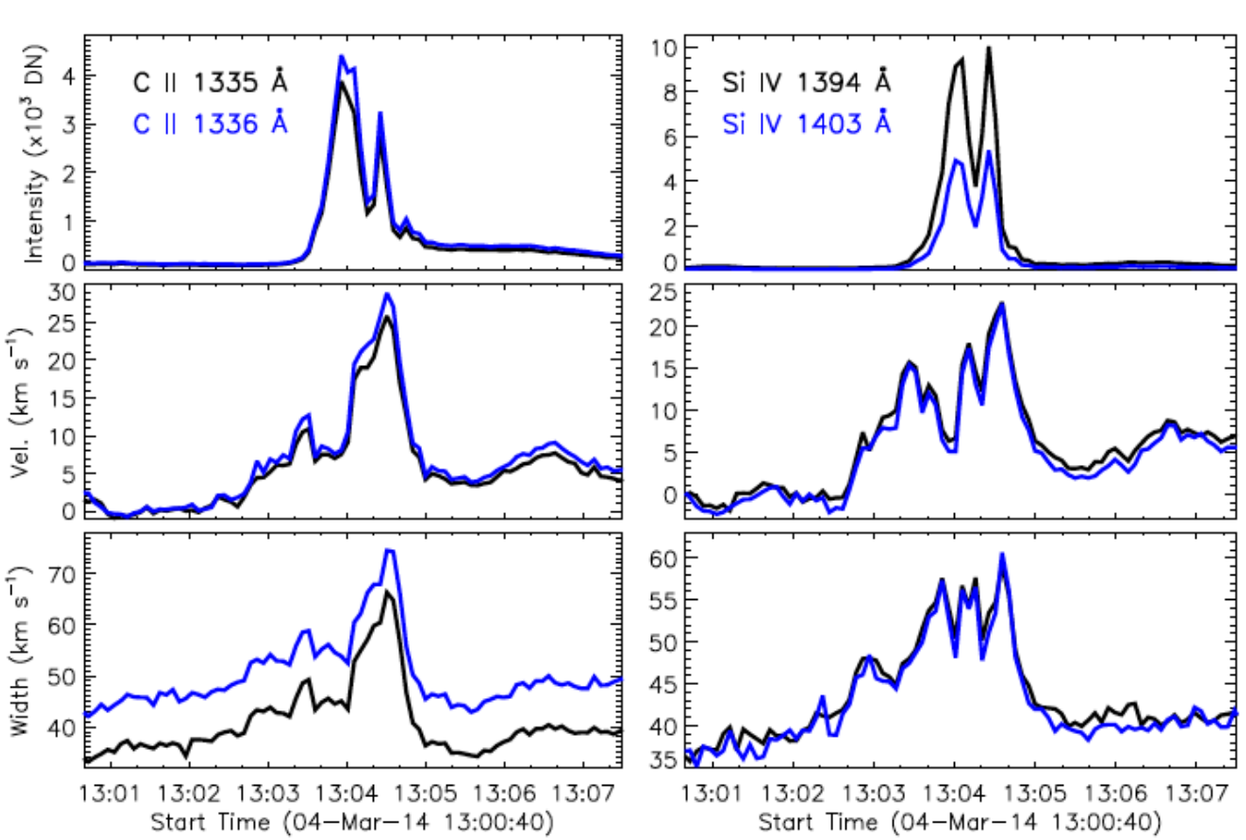

Density-sensitive line pair O IV λ1399/ λ1401

Ne =$10^{11.5}$ cm^{-3}

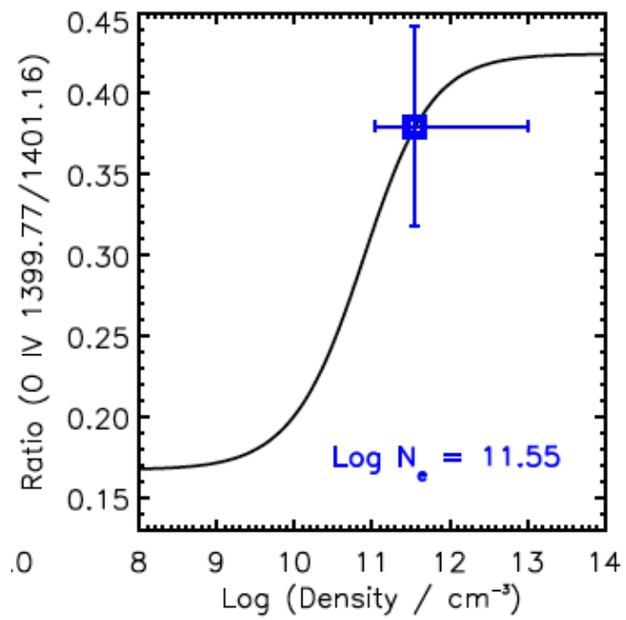

Initial signature first in line width

Polito et al. 2016

Energetics of Microflare

The thermal and kinetic energy density can be given by,

$$E_{th} = 3/2\ n_e\ k_B\ T \qquad\qquad E_{kin} = 1/2\ n_e\ \mu\ v^2$$

Energetics of Microflare

The thermal and kinetic energy density can be given by,

$$E_{th} = 3/2\ n_e\ k_B\ T \qquad\qquad E_{kin} = 1/2\ n_e\ \mu\ v^2$$

For cool transition region,

Mean molecular weight, $\mu = 0.6\ m_p$
Electron number density, $n_e = 10^{11.55}\ cm^{-3}$
Temperature, $T = 1.4x10^5\ K$
Velocity, $v = 20\ km/s$
Volume, $V = 1500x1500x1500\ km^3$ (2”x2”x2”)

Total Energy released V(Eth + Ekin) = $3.7x10^{25}$ erg

Energetics of Microflare

The thermal and kinetic energy density can be given by,

$$E_{th} = 3/2\ n_e\ k_B\ T \qquad\qquad E_{kin} = 1/2\ n_e\ \mu\ v^2$$

For cool transition region,

Mean molecular weight, $\mu = 0.6\ m_p$
Electron number density, $n_e = 10^{11.55}\ cm^{-3}$
Temperature, $T = 1.4x10^5\ K$
Velocity, $v = 20\ km/s$
Volume, $V = 1500x1500x1500\ km^3$ (2”x2”x2”)

Total Energy released V(Eth + Ekin) = $3.7x10^{25}$ erg

At hot temperature,

$n_e = 9x10^{10}\ cm^{-3}$
$T = 10\ MK$
$v = 200\ km/s$

Total energy released = $7x10^{26}$ erg

from hot AIA channels.

Cooling time of bright loop

Conduction and radiation cooling time is given by (Aschwanden 1999),

$$\tau_{cond} \approx 1.1 \times 10^{-9} n_e T_e^{-5/2} L_0^2 [s] \approx 42 \text{ s} \qquad \tau_{rad} \approx \frac{3 n_e k_b T_e}{n_e^2 \Lambda(T_e)} \approx 3607 \text{ s (60 min)}$$

where $\Lambda(T_e) \approx 10^{21.94}$ erg cm^{-3} s^{-1} for EUV loops.

For half loop length $L_0 = 11 \times 10^8$ cm, temperature $T_e = 10$ MK, and density $n_e = 10^{10}$ cm^{-3}

*Conduction cooling time matches well with life time of loop observed in **AIA 131 Å**.*

Cooling time of bright loop

Conduction and radiation cooling time is given by (Aschwanden 1999),

$$\tau_{cond} \approx 1.1 \times 10^{-9} n_e T_e^{-5/2} L_0^2 [s] \approx 42 \text{ s} \qquad \tau_{rad} \approx \frac{3 n_e k_b T_e}{n_e^2 \Lambda(T_e)} \approx 3607 \text{ s (60 min)}$$

where $\Lambda(T_e) \approx 10^{21.94}$ erg cm^{-3} s^{-1} for EUV loops.

For half loop length $L_0 = 11 \times 10^8$ cm, temperature $T_e = 10$ MK, and density $n_e = 10^{10}$ cm^{-3}

*Conduction cooling time matches well with life time of loop observed in **AIA 131 Å**.*

Combined cooling time due to both conduction and radiation is given by (Cargill 1995),

$$\tau_{cool} \approx 2.35 \times 10^{-2} \frac{L_0^{5/6}}{T_e^{1/6} n_e^{1/6}} \approx 20 \text{ min}$$

*Cooling time matches well with life time of loop observed from **AIA 335 Å**.*

1-D Hydrodynamic loop simulation

- Solar corona has high thermal conductivity and low plasma-β.
- Plasma is confined within the magnetic field lines.
- Evolution of plasma can be well demonstrated with a 1-D hydrodynamic model.

$$\frac{D\rho}{Dt} + \rho\frac{\partial}{\partial s}v = 0,$$

$$\rho\frac{Dv}{Dt} = -\frac{\partial p}{\partial s} + \rho g + \rho\nu\frac{\partial^2 v}{\partial s^2},$$

$$\frac{\rho^\gamma}{\gamma - 1}\frac{D}{Dt}\left(\frac{p}{\rho^\gamma}\right) = \frac{\partial}{\partial s}\left(\kappa\frac{\partial T}{\partial s}\right) - n^2 Q(T) + H(s,t),$$

$$p = \frac{R}{\tilde{\mu}}\rho T,$$

$$\frac{D}{Dt} \equiv \frac{\partial}{\partial t} + v\frac{\partial}{\partial s},$$

Sarkar & Walsh (2008)

1-D Hydrodynamic loop simulation

- Solar corona has high thermal conductivity and low plasma-β.
- Plasma is confined within the magnetic field lines.
- Evolution of plasma can be well demonstrated with a 1-D hydrodynamic model.

$$\frac{D\rho}{Dt} + \rho\frac{\partial}{\partial s}v = 0,$$

$$\rho\frac{Dv}{Dt} = -\frac{\partial p}{\partial s} + \rho g + \rho\nu\frac{\partial^2 v}{\partial s^2},$$

$$\frac{\rho^\gamma}{\gamma - 1}\frac{D}{Dt}\left(\frac{p}{\rho^\gamma}\right) = \frac{\partial}{\partial s}\left(\kappa\frac{\partial T}{\partial s}\right) - n^2 Q(T) + H(s,t),$$

$$p = \frac{R}{\tilde{\mu}}\rho T,$$

$$\frac{D}{Dt} \equiv \frac{\partial}{\partial t} + v\frac{\partial}{\partial s},$$

Sarkar & Walsh (2008)

- The coronal loop length = 20 Mm
- The radius of the loop = 1 Mm.
- A monolithic loop heated by microflare-like heating events at both foot-points (energy 10^{27} erg).

1-D Hydrodynamic loop simulation

- Solar corona has high thermal conductivity and low plasma-β.
- Plasma is confined within the magnetic field lines.
- Evolution of plasma can be well demonstrated with a 1-D hydrodynamic model.

$$\frac{D\rho}{Dt} + \rho\frac{\partial}{\partial s}v = 0,$$

$$\rho\frac{Dv}{Dt} = -\frac{\partial p}{\partial s} + \rho g + \rho\nu\frac{\partial^2 v}{\partial s^2},$$

$$\frac{\rho^\gamma}{\gamma - 1}\frac{D}{Dt}\left(\frac{p}{\rho^\gamma}\right) = \frac{\partial}{\partial s}\left(\kappa\frac{\partial T}{\partial s}\right) - n^2 Q(T) + H(s,t),$$

$$p = \frac{R}{\tilde{\mu}}\rho T,$$

$$\frac{D}{Dt} \equiv \frac{\partial}{\partial t} + v\frac{\partial}{\partial s},$$

Sarkar & Walsh (2008)

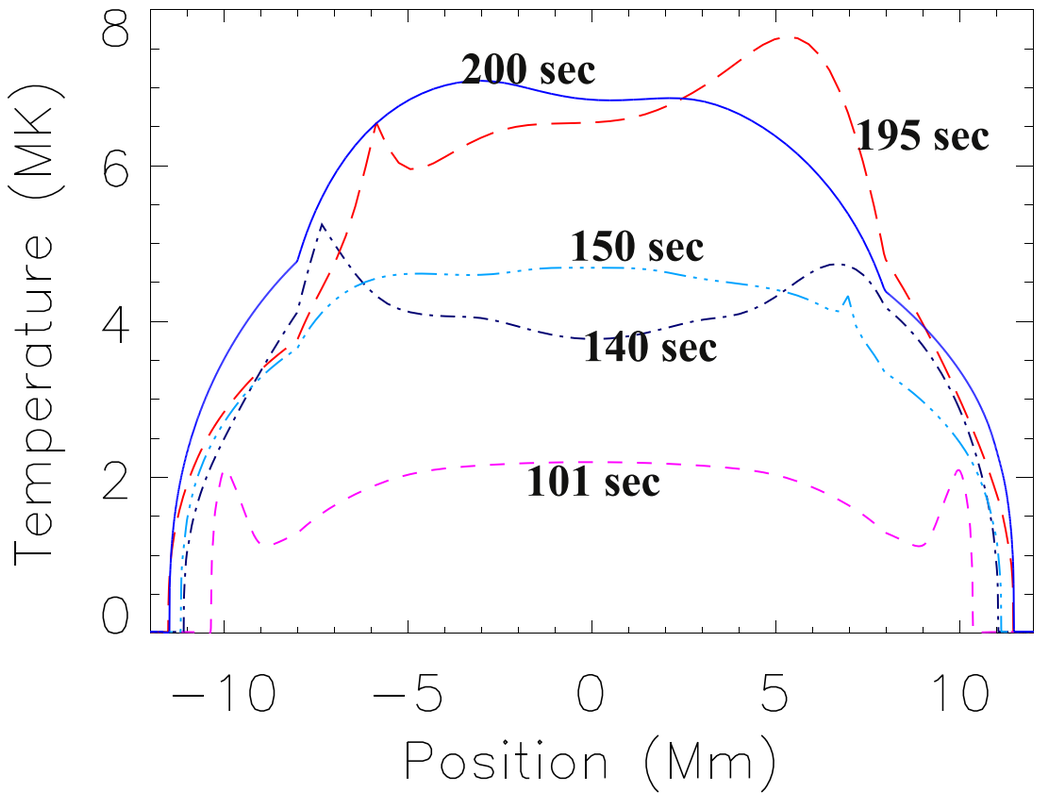

- The coronal loop length = 20 Mm
- The radius of the loop = 1 Mm.
- A monolithic loop heated by microflare-like heating events at both foot-points (energy 10^{27} erg).

Results from simulation

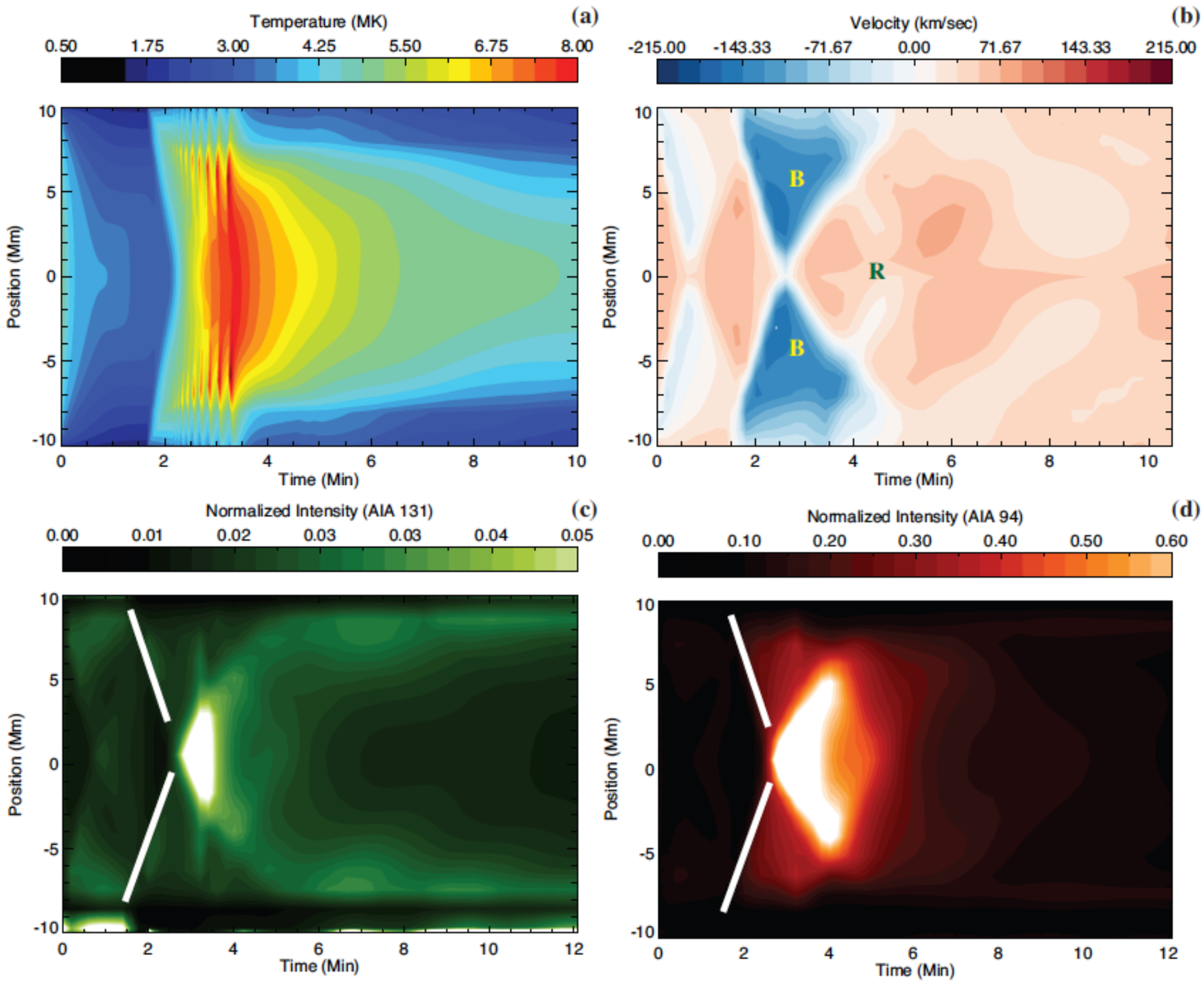

Summary

- Observed simultaneous micro-flare at two foot-points and associated loop brightening.
- Density reaches upto $10^{11.5}$ cm^{-3} whereas temperature goes upto 10 MK.
- After the micro-flare, hot plasma flows along the loop with projected speed 210 km/s, 74 km/s, and 50 km/s as measured from AIA 131 Å, 94 Å, and 335 Å passbands.
- Cool chromospheric and transition region plasma moves downwards with velocity >20 km/s.
- Observational evidence of hot mass supply to coronal loop from chromosphere because of chromospheric evaporation during micro-flare.
- Lifetime of observed hot loop is temperature dependent and that the high temperature upflows are short lived events.
- The total energy (kinetic and thermal) released during the transient is of the order of 10^{27} erg.
- Performed 1-D loop hydrodynamic simulations. Some observations were reproduced.
- A comparison of the lifetime of the loop with radiative and conductive cooling time suggests that the conduction is the dominant cooling mechanism for the loop in AIA 131 Å passband.

—Gupta, Sarkar & Tripathi, 2018, ApJ, 857, 137

Thank You